MICROWAVE DIVERSITY IMAGING OF PERFECTLY CONDUCTING OBJECT IN THE CLOSE NEAR–FIELD REGION

Tah–Hsiung Chu*, Ding–Bing Lin and Yean–Woei Kiang
Electrical Engineering Department, National Taiwan University
Taiwan, Republic of China

1. Introduction

It was known that, under physical optics approximation, Bojarski's identity forms a basis of monostatic microwave imaging a perfectly conducting object in the far–field region [1]. However, in several applications, the test object is located in the close near–field region of the receiving aperture and the paraxial approximation can not be made. The aim of this paper is to present a development of using frequency, angular and polarization diversity approaches in a close near–field microwave imaging system.

2. Theoretical Development

Considering a three–dimensional perfectly conducting object, shown in Fig.1(a) and (b) in the forward and backward scattering arrangements, is illuminated by a plane wave. Under physical optics approximation and neglecting depolarization effect, the scattered field $\bar{E}_s$ over a planar array located at z=d (forward scattering) and z=–d (backward scattering) is given as [2]

$$\bar{E}_s(x,y,z=\pm d,\bar{k}_0) = -j\omega\mu_0 \iint_{S_{ill}} 2\hat{n}\times\bar{H}_i(\bar{r}')G(|\bar{r}-\bar{r}'|)d^2\bar{r}'$$

$$= -j\omega\mu_0 H_0 \iint_{S_{ill}} 2\hat{n}\times\hat{a}_h e^{-j\bar{k}_0\cdot\bar{r}'} G(|\bar{r}-\bar{r}'|)d^2\bar{r}' \quad (1)$$

where $\bar{H}_i(\bar{r}')=H_0\exp(-j\bar{k}_0\cdot\bar{r}')\hat{a}_h$ is the incident plane wave with wave vector $\bar{k}_0=k_{x0}\hat{x}+k_{y0}\hat{y}+k_{z0}\hat{z}$ and unit vector $\hat{a}_h$ perpendicular to $\bar{k}_0$, $\bar{r}$ and $\bar{r}'$ are position vectors, $\hat{n}$ is an outward unit vector normal to the object surface. $G(|\bar{r}-\bar{r}'|)$ is the Green's function in the free space and the surface integral is over the object illuminated region S_{ill}.

Assuming the polarization state of receiving array in the direction of $\hat{p}$, the scattered field recorded by a planar array at z=d or z=–d becomes

$$U_s(x,y,z=\pm d,\bar{k}_0) = \hat{p}\cdot\bar{E}_s(x,y,z=\pm d,\bar{k}_0)$$

$$= -j\omega\mu_0 H_0 \iiint O(\bar{r}')e^{-j\bar{k}_0\cdot\bar{r}'} G(|\bar{r}-\bar{r}'|)d^3\bar{r}' \quad (2)$$

where

$$O(\bar{r}') = \hat{p}\cdot(2\hat{n}\times\hat{a}_h)\delta(S(\bar{r}')) \quad (3)$$

is defined as the object function which is related to the polarization states of the transmitting and receiving antennas and the object shape, and $\delta(\cdot)$ is a one–dimensional Dirac–delta function with its argument defined as $S(\bar{r}')=0$ as $\bar{r}'\in S_{ill}$ and $\neq 0$ elsewhere to reduce the volume integral in eq.(2) to the surface integral in eq.(1).

The plane wave expansion of Green's function in eq.(3) is given as [3]

CH2654-2/89/0000-0082 $1.00 ©1989 IEEE

$$G(|\bar{r}-\bar{r}'|) = \frac{1}{(4\pi)^2}\iint \frac{-j}{2k_x} e^{-jk_x|\pm d-z'|} e^{-j[k_x(x-x')+k_y(y-y')]} dk_x dk_y \quad (4)$$

where

$$k_z = \begin{cases} \sqrt{k_0^2-k_x^2-k_y^2} & \text{as } \sqrt{k_x^2+k_y^2} \le k_0 \\ j\sqrt{k_x^2+k_y^2-k_0^2} & \text{as } \sqrt{k_x^2+k_y^2} > k_0 \end{cases} \quad (5)$$

By substituting eq.(4) into eq.(2), and two-dimensional Fourier transforming the resulting expression of $U_s(x,y,z=\pm d,\bar{k}_0)$ in the x- and y-directions, we will obtain

$$\tilde{U}_s(k_x,k_y,z=\pm d,\bar{k}_0) = \frac{-\omega\mu_0 H_0}{2k_z} e^{-jk_z d} \tilde{O}(k_x-k_{x_0},k_y-k_{y_0},\pm k_z-k_{z_0}) \quad (6)$$

Equation (6) shows that the two-dimensional Fourier transformation of the scattered field recorded by a planar array located at z=d or z=-d (i.e., forward or backward scattering arrangement) yields a semi-spherical slice centered at $(-k_{x0},-k_{y0},-k_{z0})$ with radius k_0 in the three-dimensional Fourier space $\tilde{O}(k_x,k_y,k_z)$ of the scattering object function.

In the next section, a two-dimensional close near-field microwave imaging system is used to illustrate the theoretical development given above.

3. Two-dimensional Case

In a two-dimensional arrangement, the test object is assumed to be infinitely long in the y-direction and the receiving aperture is a linear array along x-direction located at z=d or z=-d for the forward or backward scattering arrangement. For a plane wave illumination with fixed wave vector $\bar{k}_0=k_0\hat{x}$, two semicircular slices in the object Fourier space $\tilde{O}(k_x,k_z)$, denoted by the solid lines in Fig.2(a) and (b), are accessible from the recorded scattered field.

In order to reconstruct the image of object function with high resolution, additional degrees of freedom to access the Fourier space data are required. Shown in Fig.3(a) and (b) are the results using angular diversity technique by rotating the scattering object a full 360° in small steps. By using frequency diversity technique, i.e., by stepping the frequency of the incident wave from f_1 to f_2 (or wavenumber from k_1 to k_2), the semicircular slices in Fig.2(a) and (b) will then extend to a crescent-shaped section and a fan-shaped section in the object Fourier space as shown in Fig.4(a) and (b). Therefore in the backward scattering arrangement a total of four views can fill a large portion of the object Fourier space using frequency and angular diversity techniques, while it shows more views are needed for the forward scattering arrangement as illustrated in Fig.5(a) and (b). Furthermore, by changing the polarization states of transmitting and receiving antennas (i.e., polarization diversity), different Fourier space data are accessible, and the reconstructed image for each polarization state pair gives the different feature information of the scattering object.

Numerical results of a perfectly conducting cylinder with radius 15cm in the backward scattering arrangement using frequency and angular diversity techniques are shown in Fig.6(a) and (b). The cylinder is located at z=-30cm from a 384cm long linear receiving array. The scattered field data are

sampled at 256 equally spaced points with frequency stepped from 5GHz to 10GHz in 32 steps. and the polarization states used are $\hat{a}_h=\hat{x}$ and $\hat{p}=\hat{y}$. The object Fourier space data $\tilde{O}(k_x,k_y)$ obtained from four orthogonal views are shown in Fig.6(a). The circular ring image shown in Fig.6(b) reconstructed from two–dimensional Fourier transformation represents the shape of the scattering object and is in good agreement with the object geometry.

References

[1] R.M. Lewis, "Physical optics inverse diffraction", IEEE Trans. Antenna and Propag., AP–24, pp. 308–314, 1969.

[2] R.F. Harrington, Time–Harmonic Electromagnetic Fields, McGraw–Hill, New York, 1961.

[3] E. Wolf, "Three–dimensional structure determination of semi–transparent objects from holographic data", Optical Communication, Vol. 1, pp. 153–156, 1969.

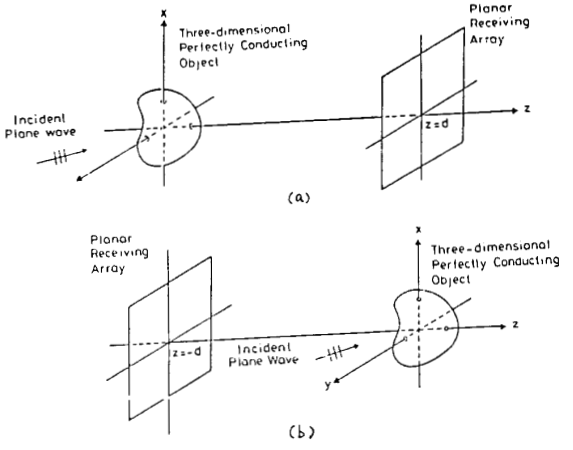

Fig.1. (a) The forward and (b) backward scattering geometries.

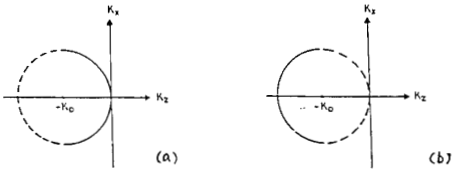

Fig.2. Object Fourier slices accessed in the (a) forward and (b) backward scattering arrangements with single frequency (wavenumber k_0) plane wave illumination.

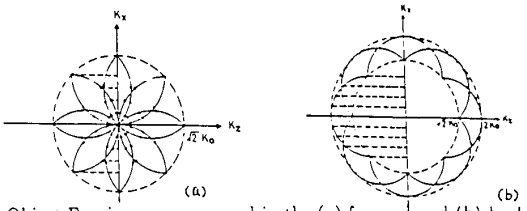

Fig.3. Object Fourier space accessed in the (a) forward and (b) backward scattering arrangements using angular diversity technique for 360° viewing angle.

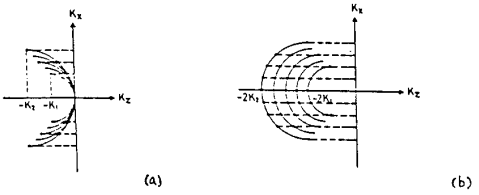

Fig.4. Object Fourier space accessed in the (a) forward and (b) backward scattering arrangements using frequency diversity technique with k_0 stepped from k_1 to k_2.

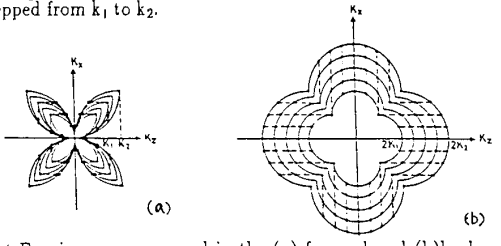

Fig.5. Object Fourier space accessed in the (a) forward and (b)backward scattering arrangements using frequency and angular diversity techniques (k_0 stepped from k_1 to k_2, and four orthogonal views).

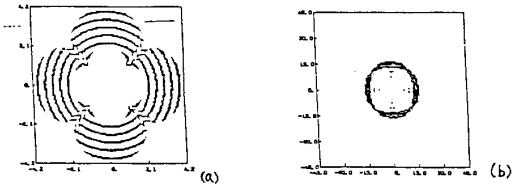

Fig.6. Results of (a) object Fourier space data of a perfectly conducting cylinder accessed in the frequency range (5–10)GHz and four orthogonal views and (b) its reconstructed image